

The numerical study of the nonlinear dynamics of a light, axially moving string

H. Koivurova*

Department of Mechanical Engineering, University of Oulu, Box 4200, FIN-90014 University of Oulu, Finland

Received 2 May 2008; received in revised form 28 July 2008; accepted 28 July 2008

Handling Editor: A.V. Metrikine

Available online 3 September 2008

Abstract

The vibration characteristics of a light axially moving band are investigated by a numerical study in the subcritical and supercritical speed ranges. Equations of motion for the geometrically nonlinear axially moving string are formulated using Hamilton's principle and discretized by the finite element method. The periodic nonlinear problem for the string is solved by the Fourier–Galerkin–Newton (FGN) method. The nonlinear dynamic behaviour of an axially moving band is examined through the dependences between the fundamental frequency, axial velocity and vibration amplitude resulting from nonlinear free vibration. In general, the behaviour of the nonlinear axially moving string is similar to that of a nonlinear beam, the most notable differences being the fact that the string does not undergo bifurcation from a straight configuration to curved equilibrium states in a supercritical transport speed regime, nor does the equilibrium state remain straight.

© 2008 Elsevier Ltd. All rights reserved.

1. Introduction

There is a large class of industrial processes which involve the transport of bands and webs across spans. From the point of view of mechanics, the translating structural members must have special characteristics with regard to vibration and dynamic stability. The topic of axially moving material has been studied widely, and recent research developments have been reviewed by Chen [1] and Païdoussis [2]. Our interest is in the topic of nonlinear vibrations in an axially moving string, which has also received much attention in the literature. The earliest known study of fundamental period nonlinear transverse vibration, by Mote [3], showed the significance of tension variation as velocity increases, while Bapat and Srinivasan [4] used the method of harmonic balance to obtain approximate period–tension relationships by the Galerkin's method and to determine the frequency of transverse oscillations for a nonlinear travelling string. Ames et al. [5] used a finite difference technique to compute the nonlinear response of a harmonically excited translating string while Kim and Tabarrok [6] resolved the nonlinear response of a travelling string using the method of characteristics. Wickert [7] studied a nonlinear translating string and beam and found that the contribution of nonlinear

*Tel.: +358 8 553 2172; fax: +358 8 553 2026.

E-mail address: Hannu.Koivurova@oulu.fi

stiffness increases with speed and grows most rapidly near critical speeds. Recently, the studies are frequently focussed to the axially moving viscoelastic strings [8–10] and the time-dependent axial velocity [11–13]. For instance, Chen et al. [10] investigated an axially travelling viscoelastic string by using the Boltzmann superposition principle along with the Galerkin method, and presented chaotic behaviours and bifurcation diagrams with varying parameters. Pakdemirli and Ulsoy presented the dynamic stability of an axially accelerating string by using the method of multiple scales [11].

Already in the earlier studies [3,5–7] it was noticed that the linear model of the system is not adequate near the critical speed, meaning here the lowest of the critical speeds defined as the speeds where the system has a vanishing eigenvalue and is subject to a divergence instability. Transport speeds above the lowest critical speed are termed supercritical. Although above observation the dynamic behaviour of an axially moving string has not been studied very intensively near critical speed or in a supercritical velocity regime. Parker [14] examined the supercritical speed dynamics of an elastically supported string with particular focus on the distribution of the critical speed and the stability of the trivial equilibrium. Some interest has been shown in supercritical velocity regimes in axially moving beams. Wickert [7] used singular perturbation techniques to examine vibration and bifurcation in both subcritical and supercritical speed ranges, while Hwang and Perkins [15,16] investigated the effect of an initial curvature due to supporting wheels and pulleys on bifurcation and the stability of equilibrium. Ravindra and Zhu [17] studied pitchfork-type bifurcation and chaos in an axially accelerating beam in a supercritical regime, and Pellicano et al. [18,19] studied post-bifurcation velocity with viscous damping and external harmonic excitation in the supercritical speed range using a high-dimensional discrete model obtained by the Galerkin procedure.

The aim of this paper is to examine the subcritical and supercritical speed dynamics of an axially moving narrow band with particular focus on free vibration and vibration shape. The equations of motion are formulated using Hamilton's principle and discretized by the finite element method. The nonlinear dynamic behaviour of the structure is investigated by analysing free and steady-state periodic vibration in the geometrically nonlinear axially moving band. The periodic nonlinear problem is solved by the Fourier–Galerkin–Newton (FGN) method according to Narayanan and Sekar [20]. The structural response to harmonic excitation and the backbone curves of free vibration show that the nonlinearities have a considerable effect on the dynamic behaviour of the system.

2. Equations of motion for a discrete axially moving string

The physical model of the system is shown in Fig. 1, a string of axial stiffness EA travels under applied tension T_0 with a constant transport speed v_a between two simple supports. The longitudinal and transverse displacements of the string are described by $u(x, t)$ and $w(x, t)$. The kinematical description of the model follows the formulation and assumptions of a taut axially moving string presented in Ref. [21] and the element development follows the model and notations introduced by Chen et al. [24] for a geometrically nonlinear beam.

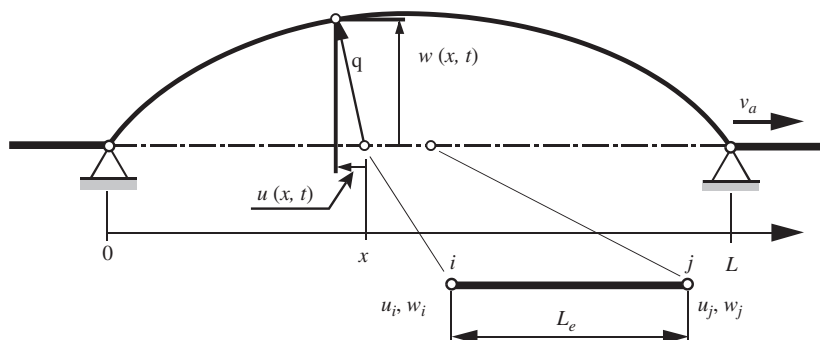


Fig. 1. Model of axially moving string.

For plane frame structural nonlinear finite element analysis, a plane axially moving string element shown in Fig. 1 is employed. The displacement vector of an point within the element are given as a function of a element displacement vector \mathbf{q}_e as

$$\mathbf{U} = \mathbf{N}\mathbf{q}_e, \tag{1}$$

$$\mathbf{U} = [u \quad w]^T, \quad \mathbf{N} = \begin{bmatrix} \mathbf{N}^s & 0 \\ 0 & \mathbf{N}^{ts} \end{bmatrix}^T \quad \text{and} \quad \mathbf{q}_e = [\mathbf{u}_e^T \quad \mathbf{w}_e^T]^T, \tag{2}$$

where $\mathbf{u}_e = [u_i \quad u_j]^T$ and $\mathbf{w}_e = [w_i \quad w_j]^T$ are nodal displacements and \mathbf{N}^s is the shape function vector defined as

$$\mathbf{N}^s = [N_1 \quad N_2] \tag{3}$$

in which $N_1 = x/L_e$, $N_2 = 1-x/L_e$ and L_e is element length.

For convenience of formulation the strain is defined as vector

$$\mathbf{E} = [\varepsilon \quad 0]^T, \tag{4}$$

where ε is axial strain including the geometrically nonlinear effect arising from the longitudinal stretching, i.e.

$$\varepsilon = \frac{\partial u}{\partial x} + \frac{1}{2} \left(\frac{\partial w}{\partial x} \right)^2. \tag{5}$$

By substituting Eq. (1) into Eq. (5), strain vector can be written as

$$\mathbf{E} = \mathbf{B}_0\mathbf{q}_e + \frac{1}{2}\mathbf{B}_L\mathbf{q}_e, \tag{6}$$

where \mathbf{B}_0 is the strain matrix coming from the linear part of the strain and \mathbf{B}_L is the strain matrix of the nonlinear elastic problem, which are, respectively

$$\mathbf{B}_0 = \begin{bmatrix} \frac{\partial \mathbf{N}^s}{\partial x} & 0 \\ 0 & 0 \end{bmatrix}, \quad \mathbf{B}_L = \begin{bmatrix} 0 & \mathbf{w}_e^T \left(\frac{\partial \mathbf{N}^s}{\partial x} \right)^T \frac{\partial \mathbf{N}^{ts}}{\partial x} \\ 0 & 0 \end{bmatrix}. \tag{7}$$

The stress–strain relationship can be written as

$$\boldsymbol{\sigma} = \begin{bmatrix} T \\ 0 \end{bmatrix} = \begin{bmatrix} EA & 0 \\ 0 & 0 \end{bmatrix} \begin{bmatrix} \varepsilon \\ 0 \end{bmatrix} = \mathbf{D}\mathbf{E}, \tag{8}$$

where the stress vector $\boldsymbol{\sigma}$ contains only the axial component, a resultant force T and constitutive matrix \mathbf{D} includes axial term, where E is the Young’s modulus and A the cross-sectional area.

The equations of two-dimensional, planar motion governing an axially moving string can be derived on Hamilton’s principle, although since the traditional form is formulated for a closed system, i.e. a system containing the same particles throughout, a mixed Lagrangian–Eulerian formulation according to Refs. [21,22] is used in this consideration, so that the motion of the system is due to the movement of the configuration and of material particles passing through it. Thus, the particles which fill the domain are assumed to be changing all the time and the energy flux across the boundaries must be taken into account. By assuming a special case in which the boundaries are fixed at both the inlet and outlet, the fluxes in and out are rendered equal and the net energy flux through the boundaries is zero. In this case, as shown by McIvar [23], Hamilton’s principle takes the familiar form

$$\delta \int_{t_1}^{t_2} (K - U + W) dt = 0, \tag{9}$$

where δ is the variation operator, K the kinetic energy, U the strain energy and W the work done by the external forces. The kinetic energy is given by

$$K = \int_0^{L_e} \mathbf{V}^T \mathbf{V} \rho A \, dx, \quad (10)$$

where ρA is the constant mass per unit length of the string and \mathbf{V} presents the velocity of a string particle. According to Refs. [21,27] the motion of a material particle consists of the movement of the configuration and the transport movement of the passing particles, i.e.

$$\mathbf{V} = \begin{bmatrix} u_{,t} + v_a(1 + u_{,x}) \\ w_{,t} + v_a w_{,x} \end{bmatrix} = \mathbf{U}_{,t} + v_a \mathbf{U}_{,x} + v_a \begin{bmatrix} 1 \\ 0 \end{bmatrix}. \quad (11)$$

The strain energy is defined as

$$U = \int_0^{L_e} \mathbf{E}^T \boldsymbol{\sigma} \, dx \quad (12)$$

and the work done by the external forces

$$W = \int_0^{L_e} \mathbf{U}^T \mathbf{P} \, dx, \quad (13)$$

where the external force vector \mathbf{P} includes axial loads $f_x(x, t)$ and transverse loads $f_y(x, t)$, i.e.

$$\mathbf{P} = \begin{bmatrix} f_x(x, t) & f_y(x, t) \end{bmatrix}^T. \quad (14)$$

By noting from Laukkanen [25] and Kulachenko et al. [22] the special features arising from the gyroscopic effects of an axially moving structure, the equation of motion for an axially moving string element can be written as

$$\mathbf{M}_e \ddot{\mathbf{q}}_e + \mathbf{C}_e \dot{\mathbf{q}}_e + \mathbf{K}_e(\mathbf{q}_e) \mathbf{q}_e = \mathbf{F}_e - \mathbf{B}_{eV}, \quad (15)$$

where \mathbf{M}_e is the mass matrix, \mathbf{C}_e the damping matrix, \mathbf{K}_e the stiffness matrix, \mathbf{F}_e the external force vector and \mathbf{B}_{eV} the inertial force vector. The consistent mass matrix is

$$\mathbf{M}_e = \rho A \int_0^{L_e} \mathbf{N}^T \mathbf{N} \, dx, \quad (16)$$

The element damping matrix consists of the damping matrix \mathbf{C}_{eD} and gyroscopic matrix \mathbf{C}_{eG} :

$$\mathbf{C}_e = \mathbf{C}_{eD} + \mathbf{C}_{eG}. \quad (17)$$

In which are, respectively

$$\mathbf{C}_{eD} = v \int_0^{L_e} \mathbf{N}^T \mathbf{N} \, dx \quad (18)$$

and

$$\mathbf{C}_{eG} = v_a \int_0^{L_e} (\mathbf{N}^T \mathbf{N}_{,x} - \mathbf{N}_{,x}^T \mathbf{N}) \, dx, \quad (19)$$

where v is the damping coefficient and v_a is the transport speed of the material. The element stiffness matrix includes the linear stiffness matrix \mathbf{K}_0 , the nonlinear stiffness matrix \mathbf{K}_{NL} and the gyroscopic stiffness matrix \mathbf{K}_G :

$$\mathbf{K}_e = \mathbf{K}_0 + \mathbf{K}_{NL} - \mathbf{K}_G, \quad (20)$$

which are, respectively

$$\mathbf{K}_0 = \int_0^{L_e} \mathbf{B}_0^T \mathbf{D} \mathbf{B}_0 \, dx, \quad (21)$$

$$\mathbf{K}_{NL} = \int_0^{L_e} \left(\frac{1}{2} \mathbf{B}_0^T \mathbf{D} \mathbf{B}_L + \mathbf{B}_L^T \mathbf{D} \mathbf{B}_0 + \frac{1}{2} \mathbf{B}_L^T \mathbf{D} \mathbf{B}_L \right) dx \quad (22)$$

and

$$\mathbf{K}_G = v_a^2 \int_0^{L_e} \mathbf{B}_G^T \mathbf{B}_G dx, \quad (23)$$

where

$$\mathbf{B}_G = \begin{bmatrix} \frac{\partial \mathbf{N}^s}{\partial x} & 0 \\ 0 & \frac{\partial \mathbf{N}^s}{\partial x} \end{bmatrix}. \quad (24)$$

The external force vector is

$$\mathbf{F}_e = \int_0^{L_e} \mathbf{N}^T \mathbf{P} dx, \quad (25)$$

and the inertial force vector is

$$\mathbf{B}_{eV} = v_a^2 \int_0^{L_e} \left[\left(\frac{\partial \mathbf{N}^s}{\partial x} \right)^T \quad 0 \right]^T dx \quad (26)$$

Following the standard assembly, the equations of motion for the assembled structure can be written as

$$\mathbf{M} \ddot{\mathbf{q}} + \mathbf{C} \dot{\mathbf{q}} + \mathbf{K}(\mathbf{q}) \mathbf{q} = \mathbf{F}(t), \quad (27)$$

where \mathbf{q} is the global displacement vector, \mathbf{M} the global mass matrix, \mathbf{C} the damping matrix, $\mathbf{K}(\mathbf{q})$ the stiffness matrix and \mathbf{F} the global force vector, which includes the inertial force vector.

3. Periodic solution for the system

The dynamic response of the system is assumed to be periodic with a frequency equal to ω . Setting the non-dimensional time as $\tau = \omega t$, the equation of motion, Eq. (27) becomes

$$\omega^2 \mathbf{M} \mathbf{q}'' + \omega \mathbf{C} \mathbf{q}' + \mathbf{K}(\mathbf{q}) \mathbf{q} = \mathbf{F}(\tau), \quad (28)$$

where the primes denote derivatives with respect to the non-dimensional time τ . The first step in the Fourier–Galerkin–Newton (FGN) method is a Newton–Raphson procedure carried out using a Taylor series [20]. Starting from a known state \mathbf{q}_0 and ω_0 , a neighbouring state is reached through a parametric incrementation

$$\begin{aligned} \mathbf{q} &= \mathbf{q}_0 + \Delta \mathbf{q}, \\ \omega &= \omega_0 + \Delta \omega. \end{aligned} \quad (29)$$

Substituting Eq. (29) into (28) and neglecting small terms of higher order, a linearized incremental equation is obtained:

$$\omega_0^2 \mathbf{M} \Delta \mathbf{q}'' + \omega_0 \mathbf{C} \Delta \mathbf{q}' + \mathbf{K}_T(\mathbf{q}_0) \Delta \mathbf{q} = \mathbf{R} - (2\omega_0 \mathbf{M} \mathbf{q}_0'' + \mathbf{C} \mathbf{q}_0') \Delta \omega, \quad (30)$$

where \mathbf{R} denotes the residual on substituting the assumed periodic solution and is

$$\mathbf{R} = \mathbf{F}(\tau) - [\omega_0^2 \mathbf{M} \mathbf{q}_0'' + \omega_0 \mathbf{C} \mathbf{q}_0' + \mathbf{K}_T(\mathbf{q}_0) \mathbf{q}_0] \quad (31)$$

and \mathbf{K}_T is the tangent stiffness matrix. Since a periodic solution is sought, the solution \mathbf{q} and its increment $\Delta\mathbf{q}$ are represented as Fourier series, i.e.

$$\begin{aligned}\mathbf{q} &= \mathbf{Q}_0 + \sum_{j=1}^M [\mathbf{Q}_{2j-1} \cos(j\tau) + \mathbf{Q}_{2j} \sin(j\tau)], \\ \Delta\mathbf{q} &= \Delta\mathbf{Q}_0 + \sum_{j=1}^M [\Delta\mathbf{Q}_{2j-1} \cos(j\tau) + \Delta\mathbf{Q}_{2j} \sin(j\tau)],\end{aligned}\quad (32)$$

where \mathbf{Q}_0 , \mathbf{Q}_j 's $\Delta\mathbf{Q}_0$ and $\Delta\mathbf{Q}_j$'s are the Fourier coefficients and M represents the number of harmonics. A similar series expansion is assumed for the incremental velocities and accelerations appearing in Eq. (32). In order to minimize the error due to the above approximation, a Galerkin procedure with harmonic weighting functions is employed. After applying the Galerkin technique with $[1, \cos \tau, \sin \tau; \dots, \cos j\tau; \sin j\tau, \dots,]$, as weighting functions, the following expression is obtained in the frequency domain [20]:

$$\bar{\mathbf{K}}\Delta\mathbf{Q} = \bar{\mathbf{R}} - \bar{\mathbf{R}}_\omega\Delta\omega, \quad (33)$$

where

$$\begin{aligned}\bar{\mathbf{K}} &= \omega_0^2\bar{\mathbf{M}} + \omega_0\bar{\mathbf{C}} + \bar{\mathbf{K}}_T(q_0), \\ \bar{\mathbf{R}} &= \bar{\mathbf{F}} - [\omega_0^2\bar{\mathbf{M}} + \omega_0\bar{\mathbf{C}} + \bar{\mathbf{K}}(q_0)]\mathbf{Q}, \\ \bar{\mathbf{R}}_\omega &= (2\omega_0\bar{\mathbf{M}} + \bar{\mathbf{C}})\mathbf{Q}.\end{aligned}\quad (34)$$

$\bar{\mathbf{M}}$, $\bar{\mathbf{C}}$, $\bar{\mathbf{K}}_T$ and $\bar{\mathbf{F}}$ are obtained either through FFT or DFT, as shown in Ref. [20]. The number of harmonics in the Fourier series is chosen according to Ref. [20] on the basis of the error estimate, which indicates the magnitude of higher harmonic coefficients of the nonlinear residual beyond the harmonic number, i.e.

$$\varepsilon_2 = \sqrt{\sum_{j=M+1}^{2M} (\overline{\mathbf{Rnl}}_{2j-1}^2 + \overline{\mathbf{Rnl}}_{2j}^2)}, \quad (35)$$

where $\overline{\mathbf{Rnl}}_j$'s are Fourier coefficients of the nonlinear part of the residual $\bar{\mathbf{R}}$ in Eq. (34). The criteria used for increasing the harmonic terms was chosen the value $\varepsilon_2 = 0.1$ suggested by Narayanan and Sekar [20], which led to numbers of harmonics between 4 and 64. The linear algebraic Eq. (33) can be solved using Newton–Raphson techniques. The nonlinear amplitude–frequency response is obtained by incrementing either the frequency ω or one component of the coefficients of \mathbf{Q} . The solution process is described in detail by Narayanan and Sekar [20]. To improve convergence, the Jacobian matrix $\bar{\mathbf{K}}$ is updated by the Broyden method during the iterations [26].

4. Results

4.1. Verification

It is quite difficult to verify the overall accuracy of the model, because there are only a few experimental results with respect to axially moving strings [5,18,19] and none of the papers tells us of all the parameters used in the experimental system. Thus, in order to verify the method even qualitatively, we mirror the description given by Pellicano et al. [19] of their experiment on the “effect of pulley eccentricity on the vibration of a power transmission belt”, in which the load, i.e. the eccentricity of the pulley (1.25×10^{-3} m), was generated by forced harmonic boundary displacements, so that the transverse displacement causes seismic excitation and

the axial displacement tension fluctuation. In order to model the eccentricity more accurately, the loadings have a phase difference of 90° . The damping of the system is modelled by means of proportional damping:

$$\mathbf{C} = \alpha \mathbf{K} + \beta \mathbf{M}, \tag{36}$$

where the constants α and β are defined using the modal damping ratio

$$\zeta = \frac{1}{2} \left(\alpha \omega_1 + \frac{\beta}{\omega_1} \right) \tag{37}$$

on the assumption that the damping arises equally from both the stiffness and the mass. The model parameters, the damping ratio and unknowns, were fitted following the experimental data on the direct resonance of the first mode at $\omega_1 = 2\pi \times 16.7$ rad/s as shown in Fig. 2. The figure indicates clearly that if the weight of the belt itself is included, the model can describe the behaviour of the experimental system. The parametric resonance founded near direct resonance of the second mode at $\Omega/(2\omega_1) = 1$ or $\omega_2 = 2\pi \times 28$ rad/s and the third mode at $\Omega/(2\omega_1) = 1.25$ are shown in Fig. 3. With the FGN model it is possible to find both the 1/2 sub-harmonic at $\Omega/(2\omega_1) = 0.93$ and the 1/3 sub-harmonic at $\Omega/(2\omega_1) = 1.19$ in the experimental data. Moreover, the model follows the nonlinear stiffening effect well as the amplitude increases. The first peak on the left at $\Omega/(2\omega_1) = 0.845$ is the third super-harmonic and was found with a much lower damping level than that chosen on the basis of the direct resonance of the first mode and used elsewhere. This super-harmonic resonance explains the behaviour of the experimental system, because the damping model used here is simple and, as noted by Pellicano et al. [19], this is a probable source of inaccuracy.

Although it is not possible to make any quantitative comparison with the experimental results, it is quite interesting to compare the results calculated here with the analytical and numerical analyses performed for an axially moving nonlinear string by Wickert [7] and an axially moving nonlinear band by Koivurova and Pramila [27]. Wickert [7] studied a travelling beam and string with a second-order perturbation solution, employing the asymptotic method of Krylov, Bogoliubov and Mitropolsky, and made comparisons with the results of numerical integration and with some other studies. Koivurova and Pramila [27] calculated the fundamental frequency of an axially moving nonlinear membrane by transient time integration.

The free vibration of an axially moving nonlinear band is considered as a function of axial velocity. For sake of clarity, the results are shown in non-dimensional form, where the frequency is presented as a proportion of the fundamental analytical frequency f_{i0} and the axial velocity as a proportion of the critical velocity $v_{a(cr)}$.

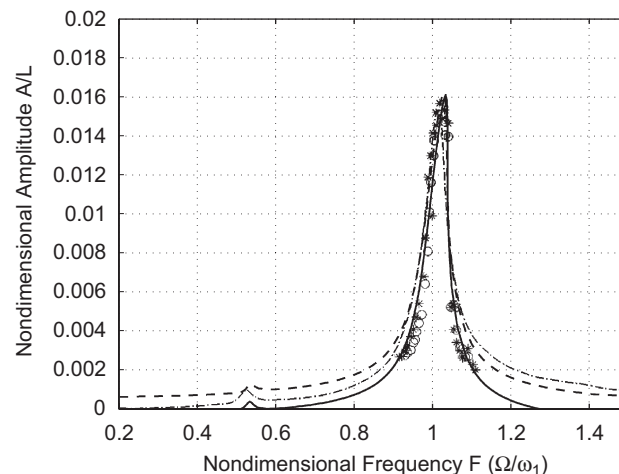


Fig. 2. Frequency amplitude curves. Primary resonance of the first mode: (- - -) according to Pellicano et al. [19]; (—) by FGN method; (- · -) by FGN method including self weight; (*) experimental results (increasing frequency Ω) and (o) experimental results (decreasing Ω) of Pellicano et al. [19].

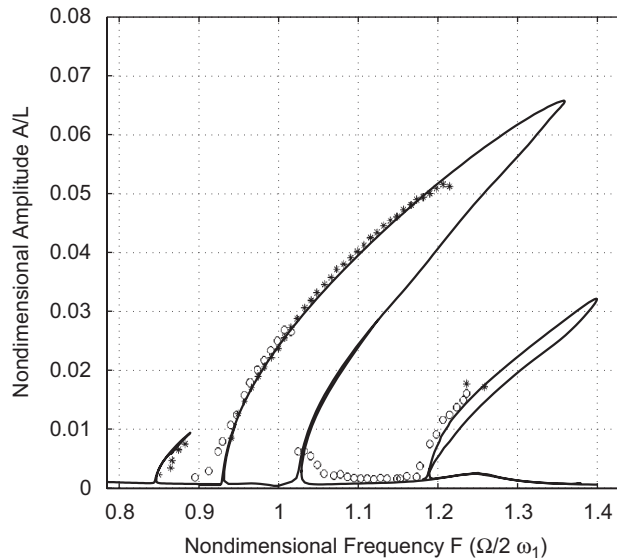


Fig. 3. Frequency amplitude curves. Parametric resonance (—) by FGN method; (*) experimental results (increasing frequency Ω) and (o) experimental results (decreasing Ω) of Pellicano et al. [19].

Table 1
Comparison of linear and nonlinear fundamental frequency calculations for a axially moving band and string with $A/L = 0.017$

Non-dimensional speed, V	0.0	0.2	0.4	0.6	0.8	1.0
Linear	1.000	0.960	0.840	0.640	0.360	0.000
Current model	1.106	1.068	0.958	0.780	0.538	0.237
FEM integration [21]	1.11	1.070	0.960	0.780	0.550	0.250
Integration [7]	1.109	1.069	0.955	0.780	0.558	0.308
Asymptotic [7]	1.112	1.077	0.966	0.792	0.569	0.308
Thurman and Mote [22]	1.103	1.067	0.955	0.770	–	–

defined as follows:

$$F = f2L\sqrt{\frac{m}{T_0}} = f/f_{10} \tag{38}$$

$$V = v_a\sqrt{\frac{m}{T_0}} = v_a/v_{a(cr)}. \tag{39}$$

The same non-dimensional presentation is used in all the subsequent analyses. The dependence between the nonlinear frequency ratio f/f_{10} and the non-dimensional vibration amplitude A/L is computed by dividing the string into 11 elements and using 16–32 harmonic terms. The parameters for the analysis are chosen so that the results of Ref. [28] are the ones given in Ref. [7] and therefore the non-dimensional vibration amplitude is 0.017 and the longitudinal stiffness parameter $v_l (= \sqrt{Eh/T_0})$ is 20. The results are listed in Table 1, where they are compared with results adapted from Refs. [7,27,28]. The present solution agrees to within 3% with both the asymptotic and numerical integration solutions [7] for $V \leq 0.8$ and [28] for $V \leq 0.6$. At higher speeds the difference increases rapidly by comparison with the results of Wickert [7]. One explanation for the difference could be the fact that a stretching approximation for longitudinal direction was used in Ref. [7], where it was proposed that the longitudinal displacement field

$$u_x(x, t) = \frac{x}{2} \int_0^l \frac{\partial u_y}{\partial x} dx - \frac{1}{2} \int_0^x \frac{\partial u_y^2}{\partial x} dx \tag{40}$$

arises entirely from finite transverse vibration. Moreover, the inclusion of nonlinearity in vibration studies is most important at near-critical speed v_{cr} , where modal stiffness is small and is dominated by the nonlinear extensional stiffness. The above conclusion is confirmed by the results of Ref. [27], which differ from the current results by about 5% at the critical speed.

Koivurova and Pramila [27] examined the nonlinear dynamic behaviour of an axially moving narrow membrane with fixed simple supports through the response to harmonic boundary excitation, calculated by direct time integration of the equations of motion. A harmonic response curve for the present nonlinear system at a non-dimensional axial velocity of 0.50 is shown in Fig. 4. The amplitude of the harmonic boundary motion is 0.0024 m and the other parameters are as follows: $L = 2.4$ m, $b = 0.47$ m, $h = 0.49$ mm, $m = 17$ g/m, $T_0 = 170$ N and $E = 1 \times 10^9$ N/m². The results given by the current model as shown in Fig. 4 are in good agreement with those reported in Ref. [27].

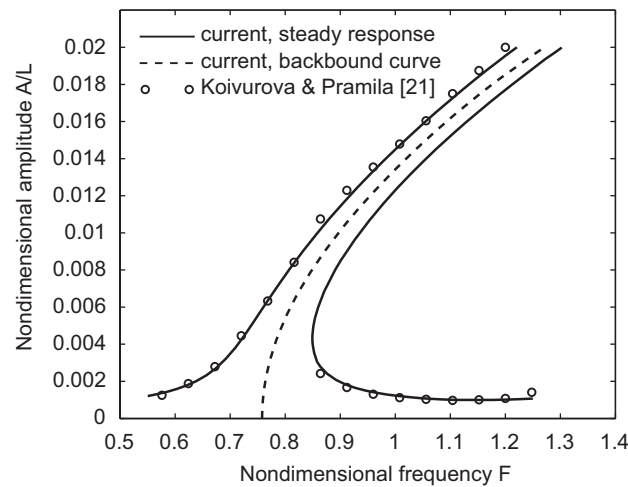


Fig. 4. Non-dimensional mid-span response amplitude for a band excited near to fundamental natural frequency. Axial velocity is 50% from the critical value.

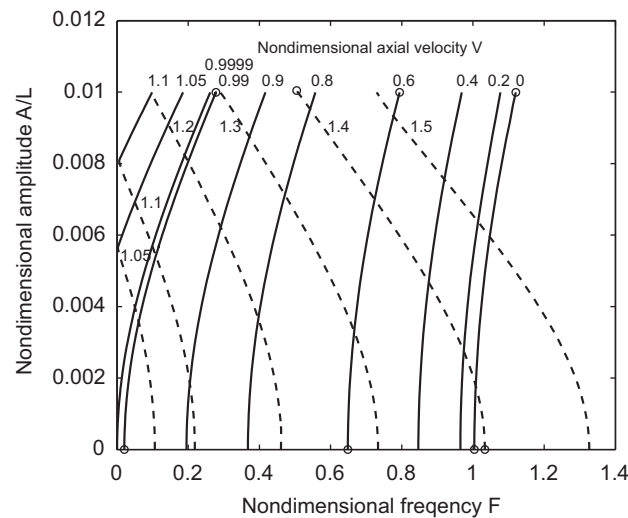


Fig. 5. Non-dimensional amplitude A/L as a function of non-dimensional fundamental frequency F with different non-dimensional axial velocities V .

4.2. Fundamental frequency of free vibration

The nonlinear dynamic behaviour of an axially moving band is examined through the dependences of fundamental frequency, axial velocity and vibration amplitude resulting from nonlinear free vibration. The parameters used are the same as in the previous application referred to above. The backbone curves describing the relation between the non-dimensional amplitude of vibration ($= A/L$) and the non-dimensional fundamental frequency with different non-dimensional axial velocity are shown in Fig. 5. The system behaves like a nonlinear hard spring at subcritical axial velocities (i.e. $0 \leq V < 1.0$) and like a soft spring at supercritical velocities ($V > 1$). The nonlinearity clearly stiffens the system in the subcritical range and softens it in the supercritical range as the amplitude is increases. This phenomenon seems to become slightly more accentuated with the increase in axial velocity, and the change is clearly visible at the supercritical velocities ($V > 1$). The figure also shows how the critical velocity increases as a function of the amplitude of free vibration. In the

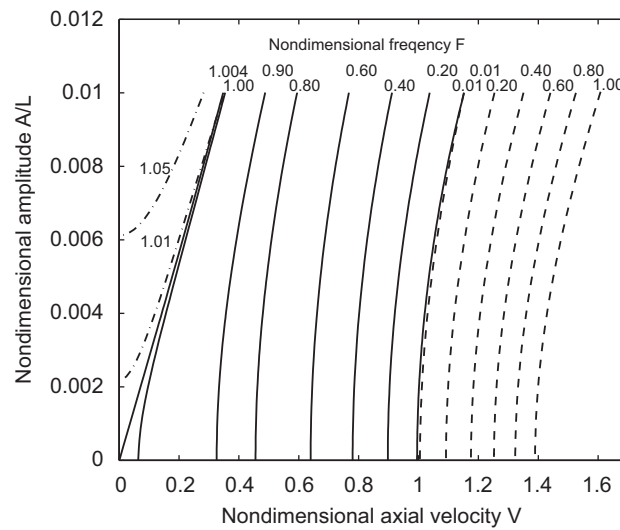


Fig. 6. Non-dimensional amplitude A/L as a function of non-dimensional axial velocity V with different non-dimensional fundamental frequencies F .

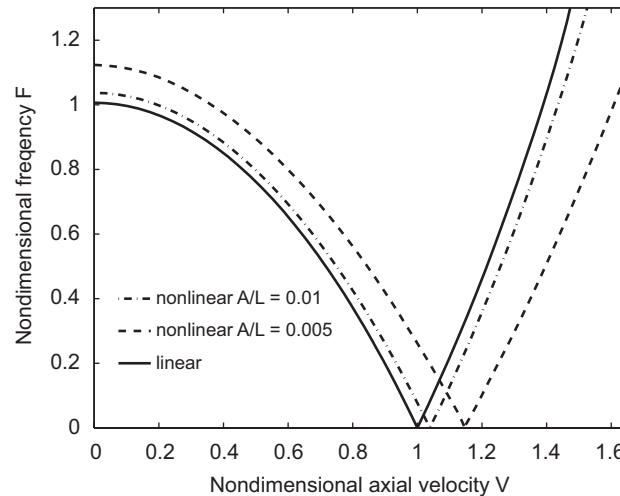


Fig. 7. Non-dimensional fundamental frequency F as a function of non-dimensional axial velocity V with different non-dimensional amplitudes A/L .

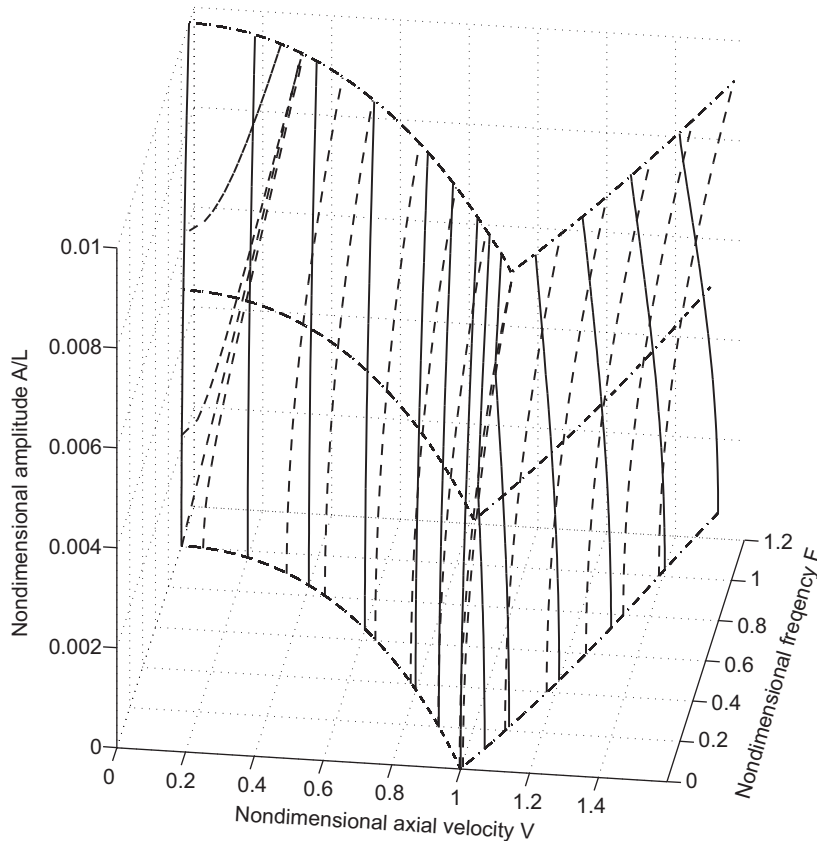


Fig. 8. Surface constructed from dependencies between non-dimensional frequency F , non-dimensional axial velocity V and non-dimensional amplitude A/L .

linear limit case at $A/L = 0$ the critical velocity $V_{(cr)} = 1.0$, from which it increases to $V_{(cr)} = 1.1$ at $A/L = 0.008$.

The relations between vibration amplitude and axial velocity at different fundamental frequencies are given in Fig. 6. Here there is no difference between the subcritical and supercritical behaviour, in that the effect of the nonlinearity bends the curves to the right, increasing the axial velocity, but instead deviant behaviour of the system is noted at lower velocities. At the frequency $F = 1.004$, which is the fundamental frequency of the linear limit ($A/L = 0$) at zero axial velocity, the dependence between the vibration amplitude and axial velocity is linear. Moreover, lower amplitude ranges cannot be obtained at frequencies higher than the above. The reason for this behaviour can be clearly seen from Figs. 7 and 8. If the frequency is over the non-movable linear fundamental limit $F = 1.004$, it is impossible to achieve linear behaviour at the lower axial velocities.

The relation between axial velocity and the fundamental frequency of free vibration is shown in Fig. 7. In general, the behaviour of a nonlinear axially moving string is similar to that of the nonlinear beam in Ref. [7], in that the linear theory underestimates stability in the subcritical range of axial velocity, overestimates it in the supercritical range and it is most limited in a near-critical regime. The most notable differences between a nonlinear string and beam are the fact that the string does not undergo bifurcation from the straight configuration to curved equilibrium states in a supercritical transport speed regime, nor does the equilibrium state remain straight. Moreover, the increase in fundamental frequency is notably quicker with a string in which the axial velocity increases than in the case of a nonlinear beam.

By combining the results shown in Figs. 5–7 we can construct a surface, as shown in Fig. 8, which describes the nonlinear dynamic behaviour of an axially moving band. The surface includes all the above dependences

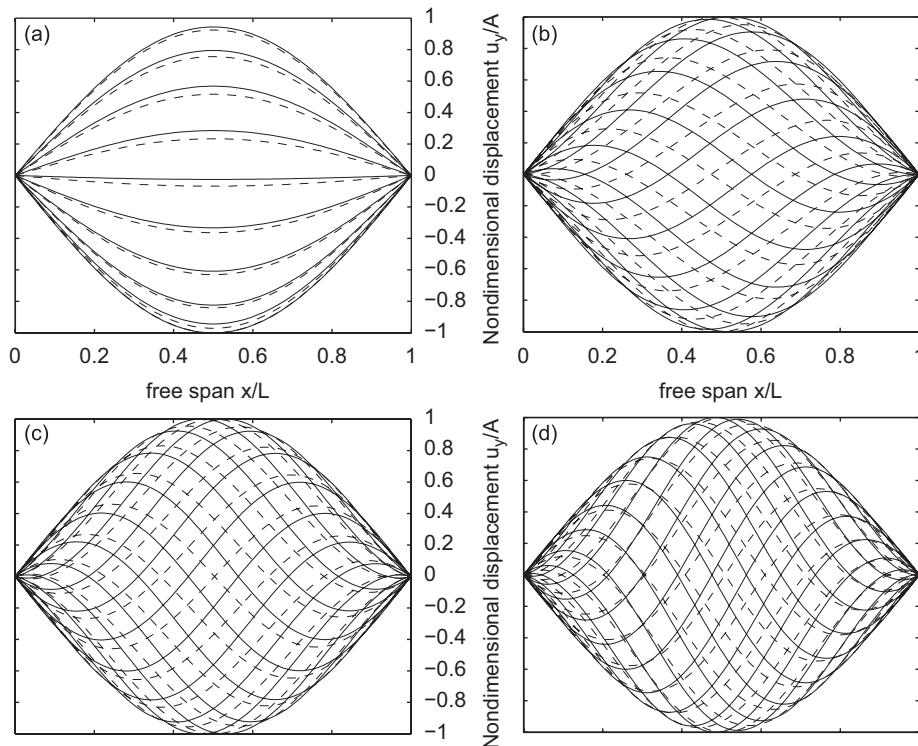


Fig. 9. Deflection shapes of the first mode of an axially moving band at axial velocities (a) $V = 0$, (b) $V = 0.60$, (c) $V = 0.99$ and (d) $V = 1.40$. At amplitude $A/L = 0.01$ (---) and linear case at $A/L \approx 0$. (—).

between fundamental frequency, axial velocity and vibration amplitude as contour lines, and therefore represents all the aspects of the behaviour of the system noted above.

The vibration modes of the fundamental frequency at three axial velocities and two amplitudes, the nonlinear $A/L = 0.01$ and the linear $A/L = 0$, are presented in Fig. 9. The modes, located as marked with ‘O’ in Fig. 5 show the characteristic behaviour of axially moving material, in that transverse vibration does not have a constant spatial phase, and therefore the material particles pass through the equilibrium at different times. This phase shift becomes more visible as the transport velocity increases and the accentuation of this phenomenon continue into the supercritical speed range. The phase shift seem to weaken with an increase in the vibration amplitude at higher velocities ($V = 0.99$ and 1.4), i.e. as the geometrically nonlinear effect increases. We can also note that exceeding of the critical velocity do not seem to affect the development of this behaviour.

5. Conclusions

The vibration characteristics of a light axially moving band are examined by the numerical study in the subcritical and supercritical speed ranges with particular focus on free vibration and the vibration shape. Equations of motion are developed on Hamilton’s principle and discretized by the finite element method. The periodic nonlinear problem for the string is solved by the FGN method. Verification of the model shows that the method is capable of describing diverse forms of behaviour in nonlinear vibrations.

The nonlinear dynamic behaviour of an axially moving band is examined through dependences between fundamental frequency, axial velocity and vibration amplitude resulting from nonlinear free vibration. The relation between the vibration amplitude and the fundamental frequency showed that increasing nonlinearity clearly stiffens the system in the subcritical range and softens it in the supercritical range. We did not find similar behaviour in the relations between vibration amplitude and axial velocity, but the subcritical and supercritical behaviour patterns were the same, in that the effect of the nonlinearity was to bend the curves to

the right with an increase in amplitude. In general, the behaviour of a nonlinear axially moving string is similar to that of a nonlinear beam as described in Ref. [7], in that the linear theory underestimates stability in the subcritical range of axial velocity, overestimates it in the supercritical range and is most limited in a near-critical regime. The most notable differences between a nonlinear string and beam are the fact that the string does not undergo bifurcation from a straight configuration to curved equilibrium states in a supercritical transport speed regime, nor does the equilibrium state remain straight.

References

- [1] L.-Q. Chen, Analysis and control of transverse vibrations of axially moving strings, *Applied Mechanics Reviews* 58 (2005) 91–116.
- [2] M.P. Paidoussis, *Fluid–Structure Interactions. Slender Structure and Axial Flow*, Elsevier Academic Press, London, 2004.
- [3] C.D. Mote Jr., On the nonlinear oscillation of an axially moving string, *Journal of Applied Mechanics* 33 (1966) 463–464.
- [4] V.A. Bapat, P. Srinivasan, Nonlinear transverse oscillations in travelling string by the method of harmonic balance, *Journal of Applied Mechanics* 34 (1967) 775–777.
- [5] W.F. Ames, S.Y. Lee, J.N. Zaiser, Non-linear vibration of a traveling threadline, *International Journal of Non-Linear Mechanics* 3 (1968) 449–469.
- [6] Y. Kim, B. Tabarrok, On the nonlinear vibration of travelling string, *Journal of the Franklin Institute* 293 (1972) 381–399.
- [7] J.A. Wickert, Nonlinear vibration of a travelling tensioned beam, *International Journal of Nonlinear Mechanics* 27 (1992) 503–517.
- [8] R.F. Fung, J.S. Huang, Y.C. Chen, The transient amplitude of the viscoelastic traveling string: an integral constitutive law, *Journal of Sound and Vibration* 201 (1997) 153–167.
- [9] L. Zhang, J.W. Zu, Non-linear vibrations of parametrically excited viscoelastic moving belts—part I: dynamic response, *Journal of Applied Mechanics* 66 (1999) 396–402.
- [10] L.Q. Chen, J.W. Zu, J. Wu, Dynamic response of the parametrically excited axially moving string constituted by the Boltzmann superposition principle, *Acta Mechanica* 162 (2003) 143–155.
- [11] M. Pakdemirli, A.G. Ulsoy, A. Ceranoglu, Transverse vibration of an axially accelerating string, *Journal of Sound and Vibration* 169 (1994) 179–196.
- [12] G. Suwken, W.T. van Horssen, On the transversal vibrations of a conveyor belt with low and time-varying velocity—part I: the string-like case, *Journal of Sound and Vibration* 264 (2003) 117–133.
- [13] J. Chung, C.S. Han, K. Yi, Vibration of an axially moving string with geometric non-linearity and translating acceleration, *Journal of Sound and Vibration* 240 (2001) 733–746.
- [14] R.G. Parker, Supercritical speed stability of the trivial equilibrium of an axially moving string on an elastic foundation, *Journal of Sound and Vibration* 221 (1999) 205–219.
- [15] S.-J. Hwang, N.C. Perkins, Supercritical stability of an axially moving beam—part I: model and equilibrium analysis, *Journal of Sound and Vibration* 154 (1992) 381–396.
- [16] S.-J. Hwang, N.C. Perkins, Supercritical stability of an axially moving beam—part II: vibration and stability analysis, *Journal of Sound and Vibration* 154 (1992) 397–409.
- [17] B. Ravindra, W.D. Zhu, Low-dimensional chaotic response of axially accelerating continuum in the supercritical regime, *Archives of Applied Mechanics* 68 (1998) 195–205.
- [18] F. Pellicano, A. Fregolent, A. Bertuzzi, F. Vestroni, Primary and parametric non-linear resonances of a power transmission belt: experimental and theoretical analysis, *Journal of Sound and Vibration* 244 (2001) 669–684.
- [19] F. Pellicano, G. Catellani, A. Fregolent, Parametric instability of belts: theory and experiments, *Computers & Structures* 82 (2004) 81–91.
- [20] S. Narayanan, S. Sekar, A frequency domain based numeric-analytical method for non-linear dynamical systems, *Journal of Sound and Vibration* 211 (1998) 409–424.
- [21] H. Koivurova, E.-M. Salonen, Comments on non-linear formulations for travelling string and beam problems, *Journal of Sound and Vibration* 225 (1999) 845–856.
- [22] A. Kulachenko, P. Gradin, H. Koivurova, Modelling the dynamical behaviour of a paper web. Part I, *Computer & Structures* 85 (2007) 131–147.
- [23] D.B. McIver, Hamilton's principle for system of changing mass, *Journal of Engineering Mathematics* 7 (1973) 249–261.
- [24] S.H. Chen, Y.K. Cheung, H.X. Xing, Nonlinear vibration of plane structures by finite element and incremental harmonic balance method, *Nonlinear Dynamics* 26 (2001) 87–104.
- [25] J. Laukkanen, FEM analysis of a travelling web, *Computer & Structures* 80 (2002) 1827–1842.
- [26] C.G. Broyden, A new method of solving non-linear simultaneous equations, *Computer Journal* 12 (1969) 94–99.
- [27] H. Koivurova, A. Pramila, Nonlinear vibration of axially moving membrane by finite element method, *Computational Mechanics* 20 (1997) 573–581.
- [28] A.L. Thurman, C.D. Mote Jr., Free, periodic, nonlinear oscillation of an axially moving strip, *Journal of Applied Mechanics* 36 (1969) 83–91.